the FEBS Journal

Dietary antioxidant curcumin inhibits microtubule assembly through tubulin binding

Kamlesh K. Gupta[1], Shubhada S. Bharne[2], Krishnan Rathinasamy[1], Nishigandha R. Naik[2] and Dulal Panda[1]

1 School of Biosciences and Bioengineering, Indian Institute of Technology Bombay, Powai, Mumbai, India
2 Biochemistry and Cell Biology, CRI, ACTREC, TMC, Kharghar, Navi Mumbai, India

Keywords
cell proliferation; curcumin; microtubule assembly dynamics; tubulin

Correspondence
D. Panda, School of Biosciences and Bioengineering, Indian Institute of Technology Bombay, Powai, Mumbai 400 076, India
Fax: +91 22 2572 3480
Tel: +91 22 2576 7838
E-mail: panda@iitb.ac.in

(Received 11 July 2006, revised 15 September 2006, accepted 4 October 2006)

doi:10.1111/j.1742-4658.2006.05525.x

Curcumin, a component of turmeric, has potent antitumor activity against several tumor types. However, its molecular target and mechanism of antiproliferative activity are not clear. Here, we identified curcumin as a novel antimicrotubule agent. We have examined the effects of curcumin on cellular microtubules and on reconstituted microtubules *in vitro*. Curcumin inhibited HeLa and MCF-7 cell proliferation in a concentration-dependent manner with IC_{50} of 13.8 ± 0.7 μM and 12 ± 0.6 μM, respectively. At higher inhibitory concentrations (> 10 μM), curcumin induced significant depolymerization of interphase microtubules and mitotic spindle microtubules of HeLa and MCF-7 cells. However, at low inhibitory concentrations there were minimal effects on cellular microtubules. It disrupted microtubule assembly *in vitro*, reduced GTPase activity, and induced tubulin aggregation. Curcumin bound to tubulin at a single site with a dissociation constant of 2.4 ± 0.4 μM and the binding of curcumin to tubulin induced conformational changes in tubulin. Colchicine and podophyllotoxin partly inhibited the binding of curcumin to tubulin, while vinblastine had no effect on the curcumin–tubulin interactions. The data together suggested that curcumin may inhibit cancer cells proliferation by perturbing microtubule assembly dynamics and may be used to develop efficacious curcumin analogues for cancer chemotherapy.

Extensive epidemiological studies in the last few decades have indicated that regular consumption of certain vegetables, fruits and spices that are known to contain cancer chemopreventive agents like quercetin, resveratrol, curcumin, and genistein can reduce the risk of cancer [1–4]. These natural dietary agents, which have negligible toxicity, can induce apoptosis in a variety of cancer cells [1–4]. Further, these agents are considered as pharmacologically safe because these are derived from natural sources that people use regularly as part of their food intake. The most studied dietary compound is curcumin (Fig. 1A), a natural polyphenolic compound originally isolated from the rhizomes of *Curcuma longa*. Curcumin has been used in Indian and Chinese traditional medicine for hundreds of years [2,3,5]. Curcumin has been shown to act as a potent anti-inflammatory and antioxidant agent [5–7]. It has generated great attention as a possible novel anticancer agent because of its encouraging antitumor activity and negligible toxicity in animal models [2–5]. Further, several clinical trials have shown that curcumin has negligible dose limited toxicity even when curcumin was administered at doses as high as 4–8 g per day [8,9]. Curcumin inhibits growth of several types of cancer cells including breast, colon, colorectal, basal cell carcinoma, and prostate cancer cells and induces apoptosis in these cells [5,7,10–13]. It

Abbreviations
DAPI, 4′,6-diamidino-2-phenylindole; DTNB, 5,5′-dithiobis(2-nitrobenzoic acid); HIF-1, hypoxia-inducible factor-1; MAP, microtubule associated protein; VEGF, vascular endothelial growth factor.

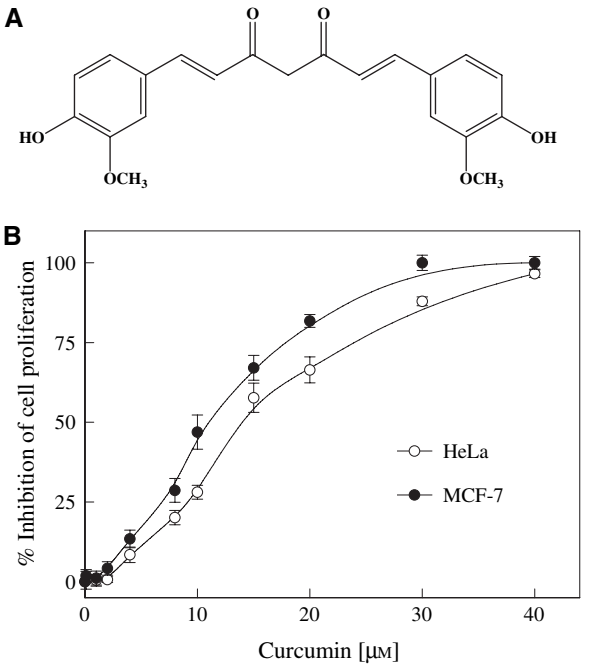

Fig. 1. Inhibition of cell proliferation by curcumin. (A) Chemical structure of curcumin [1,7-bis (4′-hydroxy-3′-Methoxyphenyl)-1,6-heptadiene-3,5-dione]. (B) Effects of curcumin on the proliferation of HeLa and MCF-7 cells were determined using sulfurhodamine B assay. Data represent mean ± SEM ($n = 6$).

has been shown to prevent tumor initiation, promotion, metastasis, and angiogenesis in experimental animals [7,14,15]. It also down regulates the expression of P-glycoprotein and increases the sensitivity of the multidrug resistant human cervical carcinoma cells (KB-V1) towards vinblastine [16]. Although curcumin possesses a broad range of anticancer activities, its molecular mechanism of action and primary cellular target(s) in cancer cells are not clear. Curcumin has been shown to arrest the cells in G_2-M phase in various cancer cells and to disrupt the mitotic spindle structure in breast cancer cells [5,10,12,17–19]. Recently, curcumin has been shown to alter the expression of many genes, which are crucial for the G_2-M transition, including tubulin and p53 suggesting that curcumin might act as an antimicrotubule agent [19]. These reports encourage us to investigate the effects of curcumin on the microtubule cytoskeleton.

Microtubules are highly dynamic polymers made up of αβ-tubulin dimers and they are essential for a variety of biological functions, especially in governing the segregation of chromosomes during mitosis [20,21]. Microtubules are considered to be very important targets for developing chemotherapeutic drugs [21,22]. Many microtubule targeted agents including taxol, vincristine, vinblastine and estramustine have been successfully used in the treatment of various forms of cancers [21,22]. These agents perturb microtubule polymerization dynamics and arrest cells at mitosis. A large body of evidence indicates that sustained mitotic block by microtubule targeted drugs triggers cell killing by apoptosis [21,22]. However, these drugs also cause severe side-effects in the patients by targeting the normal dividing cells. In addition to severe harmful side-effects, poor bioavailability and the development of drug resistance limit their application [21,23]. For example, taxol and vinblastine act as substrates for multidrug resistance protein P-glycoprotein, which also limit its efficacy [23]. So, the development of novel agents that bind to tubulin but show negligible toxicity would strongly improve the chemotherapeutic potential in the treatment of cancer. While searching for novel anticancer agents, we reasoned that curcumin could be potentially useful in the treatment of cancers because of its lack of toxicity and its broad range of antitumor activity including its strong antiangiogenic properties.

In this study, we found that curcumin inhibited proliferation of HeLa and MCF-7 cells and depolymerized interphase and mitotic microtubules of both the cell types. *In vitro*, curcumin was found to bind to tubulin, induced tubulin aggregation and perturbed microtubule assembly. The evidence presented in this study suggests that curcumin inhibits cell proliferation and triggers cell killing at least partly by perturbing microtubule assembly and function through tubulin binding. Its antimicrotubule activity as reported in this study, its limited harmful side-effects as documented by several investigators [2,8,9] and its ability to down regulate P-glycoprotein expression [23] together strongly suggest that curcumin alone or in combination with other antimicrotubule agents may be evaluated for its clinical potential against several types of cancers.

Results

Effects of curcumin on HeLa and MCF-7 cell microtubules

Curcumin inhibited proliferation of HeLa and MCF-7 cells with IC_{50} values of 13.8 ± 0.7 μM and 12 ± 0.6 μM, respectively (Fig. 1B). Under similar conditions, vinblastine and colchicine inhibited HeLa cell proliferation with IC_{50} values of 2 ± 0.2 nM and 14 ± 2 nM, respectively. Curcumin was previously shown to inhibit cell cycle progression at G_2-M and to induce apoptosis [5,10,12,17–19]. Because many cytotoxic drugs induce G_2-M arrest by targeting microtubules [21,22,24,25], we wanted to examine whether curcumin also targets microtubules. The effects of

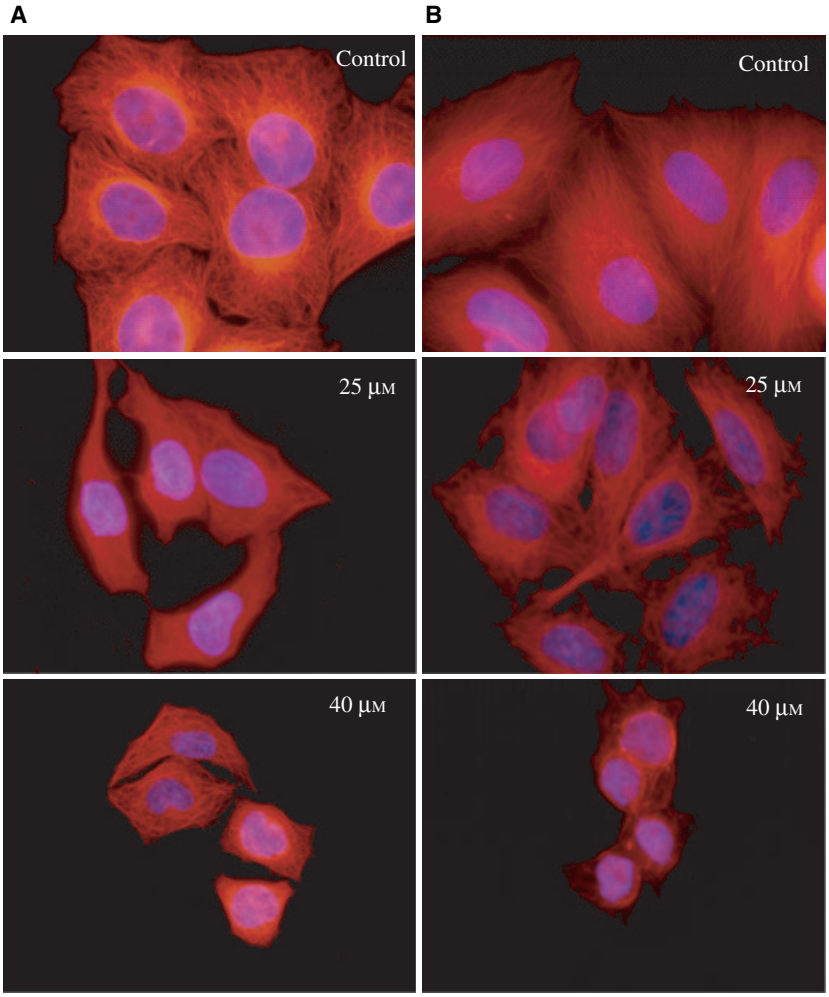

Fig. 2. Curcumin depolymerized interphase microtubules of HeLa and MCF-7 cells. Effects of 25 and 40 μM curcumin on microtubule networks of HeLa (A) and MCF-7 (B) cells are shown. Control indicates vehicle (0.1% dimethylsulfoxide) treated cells. Microtubule (red) and nucleus (blue) are shown.

curcumin on the interphase microtubules of HeLa and MCF-7 cells were examined using immunofluorescence microscopy (Fig. 2). Control cells showed typical interphase microtubule organization. No effect of curcumin on the interphase microtubule network was apparent at curcumin concentrations below 10 μM. However, at relatively higher curcumin concentrations (≥ 25 μM), a significant reduction of microtubule density occurred in both the cell types. A significant reduction in the number of microtubules at the periphery of the cells was apparent and the central networks were disorganized. For example, 25 μM curcumin that inhibited HeLa cell proliferation by ≈78% significantly depolymerized interphase microtubules. Curcumin (40 μM) strongly depolymerized interphase microtubule in both the cell types.

The effects of curcumin on the mitotic spindle organization of HeLa and MCF-7 cells are shown in Fig. 3. Control metaphase cells exhibited normal bipolar mitotic spindle organization with two prominent poles (arrow). Further, in control cells chromosomes were compact and properly aligned at the metaphase plate. Curcumin perturbed microtubules and chromosome organization in the spindle. For example, 10 μM curcumin, which inhibited proliferation of HeLa and MCF-7 cells by ≈28% and ≈46%, respectively, exerted strong disrupting effects on the spindle microtubules in both the cell types. The spindle apparatus appeared to be collapsed in the presence of curcumin. Curcumin-treated mitotic cells contained significantly shorter and fewer microtubules compared to vehicle-treated cells. Curcumin also induced aggregation of tubulin in the cells. In addition, it disorganized chromosome alignment at the metaphase plates and the condensed chromosomes appeared ball-shaped in the presence of 10 μM curcumin. Thus, curcumin depolymerized spindle microtubule organization and disorganized metaphase plate of chromosomes at lower concentrations than that was required to disrupt interphase microtubules.

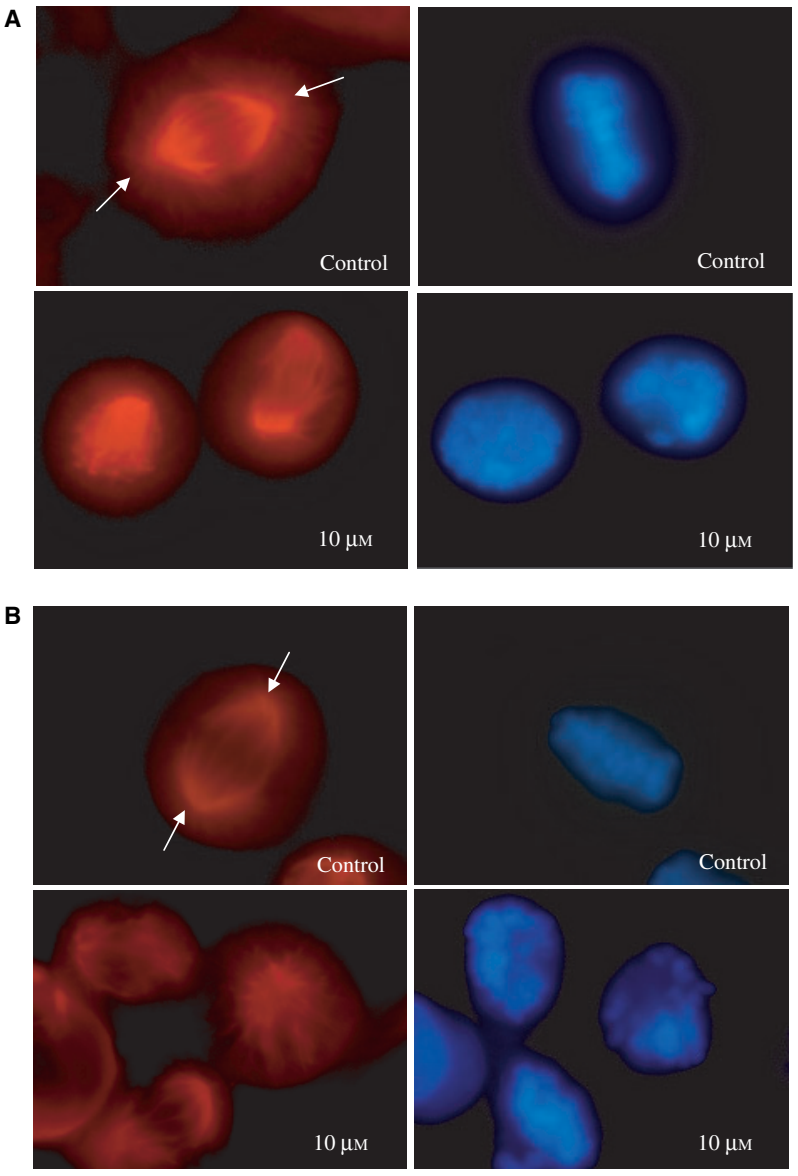

Fig. 3. Curcumin disrupts mitotic spindle organization. Effects of 10 μM curcumin on microtubules and chromosome organization of HeLa (A) and MCF-7 (B) cells are shown.

Inhibition of tubulin assembly into microtubules and induction of tubulin aggregation by curcumin *in vitro*

Because curcumin depolymerized microtubules in HeLa and MCF-7 cells, we examined the effects of curcumin on microtubule polymerization *in vitro*. We used two complementary approaches, light scattering and sedimentation, to analyze the ability of curcumin to inhibit polymerization of phosphocellulose-purified tubulin into microtubules *in vitro*. Curcumin inhibited the rate and extent of the light scattering signal of tubulin assembly in a concentration dependent manner (Fig. 4A). For example, 50 μM curcumin decreased the final extent of the light scattering signal of tubulin assembly by ≈35%, while 100 μM curcumin reduced it by ≈59% indicating that it inhibits tubulin assembly.

The effect of curcumin on the mass of assembled polymers was determined by sedimentation. Curcumin did not reduce the mass of sedimentable tubulin polymers (Fig. 4B). Similar results were obtained when polymerization was carried out with purified tubulin in the presence of glycerol, dimethylsulfoxide, Taxol, microtubule associated proteins (MAPs), or glycerol seeds (data not shown).

The extent of light scattering signal depends on the size and shape of the polymers [26]. Therefore, the decrease in the light scattering signal of tubulin assembly

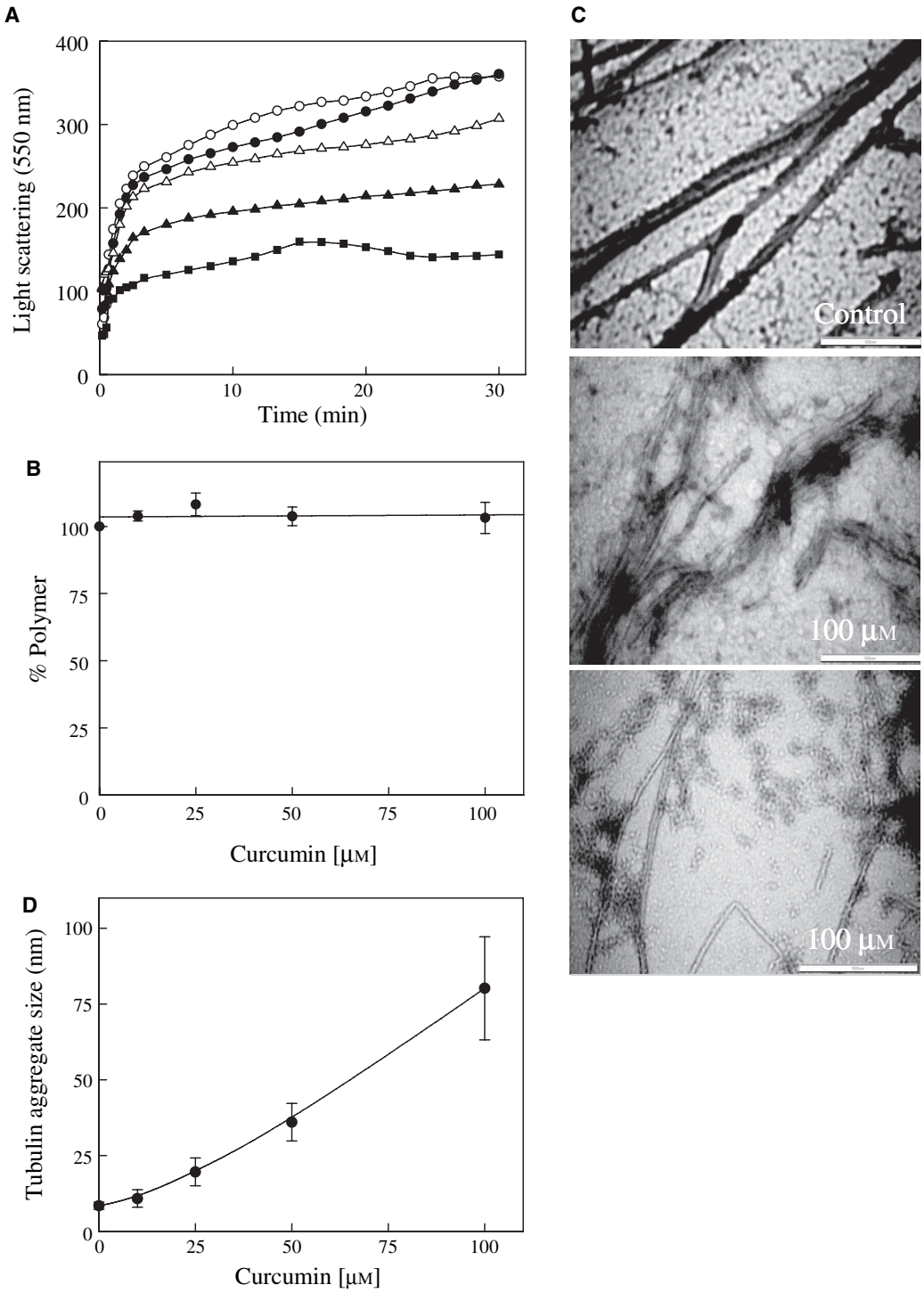

Fig. 4. Inhibition of microtubule assembly by curcumin *in vitro*. (A) Effect of curcumin on microtubule polymerization kinetics was assessed by monitoring the increase in light scattering at 550 nm. Control (○), 10 (●), 25 (△), 50 (▲), and 100 (■) μM curcumin. Data are the average of three independent experiments. (B) Curcumin did not change the sedimentable polymer mass appreciably. Data shown is mean ± SEM ($n = 4$). (C) Microtubules in the absence and presence of curcumin as visualized by electron microscopy. Images were taken at 43 000× magnification. (D) Curcumin induced association of tubulin dimers (10 μM) was monitored using dynamic light scattering at 90°. Data are mean ± SEM ($n = 4$).

in the presence of curcumin could be due to the formation of very short microtubules, altered polymer morphology or formation of small aggregates of tubulin. To distinguish among these possibilities, polymers formed in the presence of curcumin were examined by electron microscopy. Consistent with previous reports [27], tubulin polymerized in the presence of 1 M glutamate formed mainly open sheets of parallel protofilaments (Fig. 4C). In the presence of 100 μM curcumin, peeling of protofilaments was observed and large protofilaments were fragmented into small protofilaments. In addition, aggregates of tubulin were found to be abundant in the presence of 100 μM curcumin (Fig. 4C). Curcumin induced aggregation of tubulin dimers was further shown by dynamic light scattering (Fig. 4D). In the absence of curcumin, the size of a tubulin dimer was found to be 8.4 ± 1.8 nm. Incubation of tubulin with different concentrations of curcumin increased the size of the aggregates. For example, the sizes of the tubulin oligomers were found to be 19 ± 5 nm, 36 ± 6 nm and 80 ± 17 nm in the presence of 25, 50, and 100 μM curcumin, respectively.

Copolymerization of curcumin into tubulin polymer

The sedimented protein polymers were yellowish in color, suggesting that the polymers and aggregates that were formed in the presence of curcumin might be composed of tubulin–curcumin complexes. To analyze whether curcumin could incorporate into the tubulin polymer as tubulin–curcumin complex, we first prepared pure tubulin–curcumin complexes as described below. Then, tubulin was polymerized in the presence of low concentrations (1–6 μM) of tubulin–curcumin complex. At this concentration range, curcumin did not induce detectable depolymerization and aggregation of tubulin dimers. Tubulin–curcumin complex was found to be incorporated into the polymers in a concentration dependent fashion (Fig. 5A). The stoichiometries of curcumin incorporation per tubulin dimer in the microtubule were found to be 0.11 ± 0.03 and 0.32 ± 0.05 in the presence of 1 and 6 μM of curcumin, respectively. The results suggest that incorporation of curcumin in the microtubule altered polymer morphology and perturbed microtubule assembly dynamics.

Inhibition of GTP hydrolysis and induction of conformational changes in tubulin by curcumin

Many microtubule-targeted agents inhibit the functions of microtubules by modulating its GTPase activity

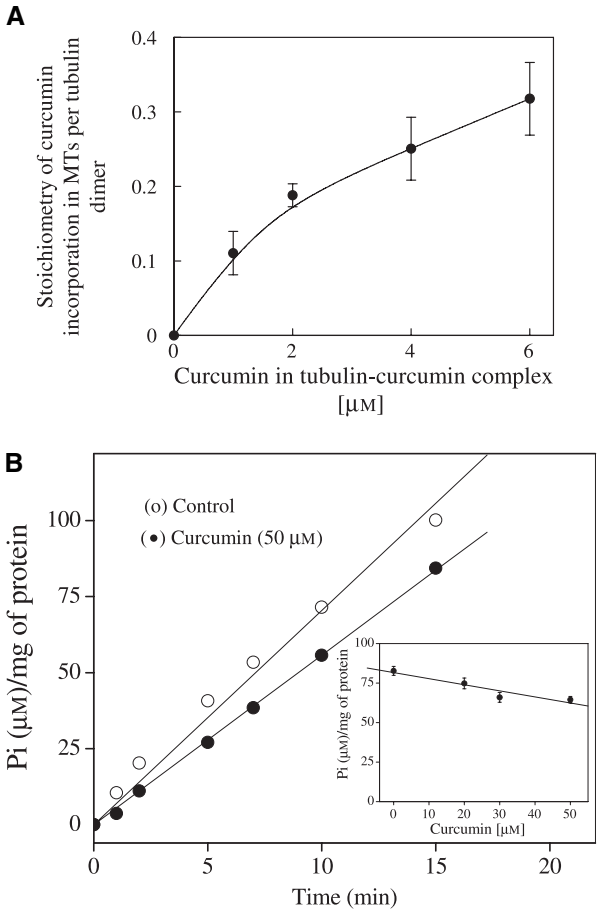

Fig. 5. Curcumin copolymerized into microtubule and inhibited GTP hydrolysis. (A) Curcumin was incorporated into the microtubules along with tubulin. Data represent mean ± SEM ($n = 4$). (B) Curcumin inhibited the rate of GTP hydrolysis of microtubule polymerization ($n = 11$). Inset shows GTP hydrolysis at various curcumin concentrations. Data are mean ± SEM ($n = 8$). Microtubule protein (1.8 mg·mL^{-1}) was polymerized in the absence and presence of 50 μM curcumin as described in Experimental procedures.

during assembly [21,25]. Curcumin inhibited the GTP hydrolysis rate of microtubule protein (tubulin plus MAPs), albeit modestly (Fig. 5B). For example, 50 μM curcumin reduced the rate of GTP hydrolysis of microtubules by 21% from 7.1 ± 0.4 to 5.6 ± 0.5 μM mg^{-1}·min^{-1}, respectively ($P < 0.01$). Further, the extent of GTP hydrolysis was inhibited by ≈22% in the presence of 50 μM curcumin ($P < 0.01$) (Fig. 5B, inset).

The sulfhydryl groups of tubulin are sensitive markers for studying tubulin conformational changes upon ligand binding [24,25]. The effect of curcumin on the conformation of tubulin was determined by using the cysteine modifying agent 5,5′-dithiobis(2-nitrobenzoic acid) (DTNB). Curcumin reduced the number of

cysteine residues accessible to DTNB; there were 13.2 ± 0.2 sulfhydryl residues accessible per tubulin dimer in the absence of curcumin and 11.7 ± 0.4 residues per tubulin dimer in the presence of curcumin. The difference in the number of modified cysteine residues in the absence and presence of curcumin was 1.5 ($P < 0.01$) indicating that the binding of curcumin to tubulin induces a conformational change in the tubulin.

Binding of curcumin to tubulin

Curcumin has weak fluorescence in neutral aqueous buffer with an emission maxima at 540 nm (Fig. 6A). When, curcumin was mixed with tubulin in a 1 : 1 molar ratio, its fluorescence intensity increased markedly (Fig. 6A). For example, the fluorescence intensity of 5 μM curcumin increased several-fold in the presence of equimolar concentration of tubulin. The emission spectrum of curcumin showed a blue-shift of 45 nm upon binding to tubulin indicating that curcumin binds to a hydrophobic region of tubulin. Figure 6B shows the titration curve of a constant amount of tubulin treated with various concentrations of curcumin. Scatchard analysis of the data yielded a linear plot with a dissociation constant of 2.4 ± 0.4 μM and a stoichiometry of 0.6 ± 0.02 (Fig. 6B, inset). The binding of curcumin to tubulin was also investigated by measuring the effects of curcumin on the intrinsic tryptophan fluorescence of tubulin. As shown in Fig. 6C, curcumin reduced the intrinsic tryptophan fluorescence of tubulin in a concentration-dependent manner. The double reciprocal plot of the binding data (Fig. 6C, inset) yielded a dissociation constant of 3.2 ± 0.5 μM, which is in excellent agreement with the K_d obtained by the curcumin fluorescence titration.

Characterization of the binding site for curcumin

We used the curcumin–tubulin complex fluorescence to determine whether curcumin could bind to the colchicine or vinblastine site on tubulin. We reasoned that if either drug could inhibit the binding of curcumin to tubulin, it should decrease the development of curcumin–tubulin complex fluorescence. The extent of curcumin binding at various concentrations of colchicine and podophyllotoxin is shown in Fig. 7A. Both colchicine and podophyllotoxin inhibited the fluorescence of tubulin–curcumin complex modestly. For example, 25 μM colchicine inhibited curcumin binding to tubulin by ≈21% and similar inhibition of curcumin fluorescence was also observed when podophyllotoxin was used in the place of colchicine. These data

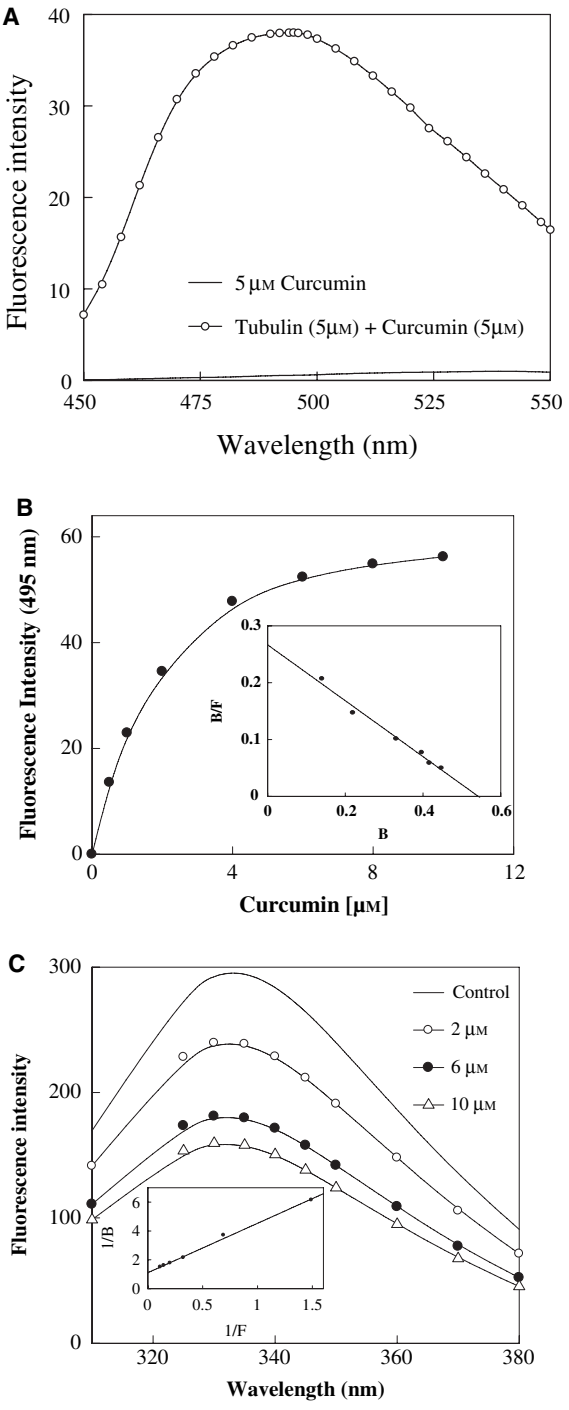

Fig. 6. Characterization of curcumin binding to tubulin. (A) Change in fluorescence spectra of curcumin after binding to tubulin (2 μM). Excitation wavelength was 425 nm. (B) Curcumin binding to tubulin was measured by fluorescence spectroscopy. The inset shows a Scatchard plot of curcumin binding to tubulin ($n = 7$). (C) Curcumin reduced the intrinsic tryptophan fluorescence of tubulin (2 μM). One of the four experiments is shown. The excitation wavelength was 295 nm. Inset shows the double reciprocal plot of binding of curcumin to tubulin ($n = 4$).

indicated that the binding site of curcumin on tubulin may partly overlap with the binding site of colchicine and podophyllotoxin. Alternatively, the binding of colchicine or podophyllotoxin to tubulin induced conformational changes in tubulin that reduced curcumin binding to the protein. In support of the second possibility, curcumin was found to bind to the preformed tubulin–colchicine or tubulin–podophyllotoxin complex (Fig. 7B). Further, 100 μM colchicine or podophyllotoxin could not displace curcumin from the preformed tubulin–curcumin complex significantly. For example, incubation of 100 μM colchicine or podophyllotoxin with the preformed tubulin–curcumin complex for 1 h at 37 °C reduced the fluorescence intensity of the preformed tubulin–curcumin complex only by 17% and 4%, respectively. Vinblastine did not affect the tubulin–curcumin complex fluorescence indicating that curcumin binding site was different from the vinblastine binding site (Fig. 7C).

Discussion

In the present study, we found that the antiproliferative activity of curcumin correlates well with its ability to depolymerize cellular microtubules. At its lowest effective inhibitory concentration (at or near IC_{50}) range, curcumin strongly depolymerized mitotic microtubules of both HeLa and MCF-7 cells. At its higher effective concentration range ($2 \times IC_{50}$), curcumin depolymerized interphase microtubules of both the cell types. *In vitro*, curcumin bound to tubulin with high affinity (K_d, 2.4 ± 0.4 μM), inhibited tubulin assembly into microtubules, reduced GTPase activity and induced aggregation of tubulin dimers.

Curcumin was found to be incorporated into microtubules in high stoichiometry (Fig. 5A) indicating that curcumin does not inhibit microtubule assembly by the 'end poisoning mechanism' as described for colchicine and vinblastine [21]. Although colchicine and podophyllotoxin partly inhibited curcumin binding to tubulin, the results obtained in this study indicate that these agents inhibit microtubule polymerization by a different molecular mechanism than that of curcumin. There are several possible mechanisms through which curcumin could inhibit microtubule polymerization. One possibility is that curcumin–tubulin complex gets incorporated into the microtubule lattice in large numbers and the incorporation of curcumin into the polymers alters the geometry of the microtubules that inhibits assembly. Another possibility is that curcumin induces conformational change in the microtubule, which alters its association with other accessory proteins. Alternatively, curcumin can sequester tubulin

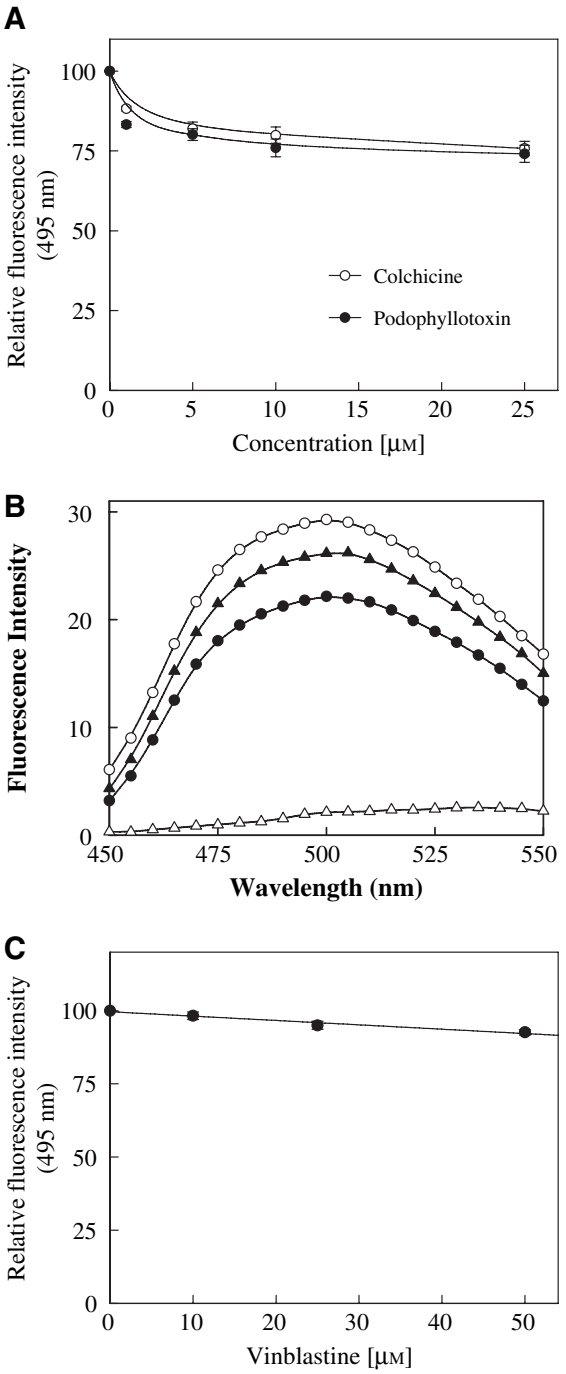

Fig. 7. Competition of curcumin with microtubule inhibitors for tubulin binding. (A) Colchicine and podophyllotoxin weakly inhibited binding of curcumin to tubulin. Data represent mean ± SEM ($n = 4$). (B) Binding of curcumin to the preformed tubulin–colchicine or tubulin–podophyllotoxin complex. Shown are emission spectra of free curcumin (△), tubulin plus curcumin (○), tubulin–colchicine complex plus curcumin (●) and tubulin–podophyllotoxin complex plus curcumin (▲). (C) Vinblastine did not inhibit the binding of curcumin to tubulin. Data are average of three independent experiments.

dimers and the sequestration of tubulin reduces free tubulin concentration for microtubule formation.

Several antimicrotubule agents such as noscapine, estramustine, cematodin and griseofulvin did not inhibit polymer mass significantly but they were shown to suppress microtubule dynamics strongly [28–31]. Curcumin perturbed microtubule assembly, reduced GTPase activity of microtubules, induced aggregation of tubulin dimers, and depolymerized both interphase and mitotic microtubules in cells indicating that curcumin may perturb microtubule dynamics. Further, 2-Methoxyestradiol is also known to copolymerize into microtubules stoichiometrically without affecting the microtubule polymer mass appreciably [32], indicating that both 2-Methoxyestradiol and curcumin might affect the microtubule assembly dynamics in a similar manner.

Curcumin is also shown to be a potent inhibitor of angiogenesis, an essential process in growth and metastasis of solid tumors [14,15]. This process requires migration, proliferation, and capillary formation by endothelial cells. Endothelial cells are stimulated by hypoxia-inducible factor-1 (HIF-1) and vascular endothelial growth factor (VEGF), and also active involvement of cytoskeleton [14,33]. Agents that inhibit the activity of HIF-1 and VEGF are considered as a potential antiangiogenic agent [33]. More recently, Mabjeesh *et al*. found that the disruption of the interphase microtubule cytoskeleton by 2-Methoxyestradiol inhibited HIF-1 activity [34]. Although the exact mechanism of antiangiogenic action of curcumin is not known, it has been suggested that curcumin inhibits angiogenesis by inhibiting HIF-1 and VEGF production in tumor cells [14,35]. We found that curcumin depolymerized interphase microtubules of both MCF-7 and HeLa cells. Thus, similar to 2-Methoxyestradiol [34], curcumin may also inhibit HIF-1 activity by perturbing microtubule assembly.

Curcumin is known to have a broad spectrum anticancer activity and it perturbs numerous signaling pathways [3–5,35]. Although curcumin was found to perturb microtubule assembly in cells and *in vitro* by binding to tubulin, the data presented in the study cannot exclude the involvement of other cellular targets for curcumin. The role of microtubules in signal transduction and intracellular transport are widely accepted. Hence, it would be reasonable to think that the modulation of the signaling pathways in cancer cells by curcumin may involve microtubule perturbation.

In brief, the study shows that curcumin inhibits microtubule assembly in HeLa and MCF-7 cells by perturbing microtubule assembly dynamics. Our findings support the development of curcumin and its analogs as novel anticancer agents for the treatment of several types of cancer including breast and cervical cancers.

Experimental procedures

Chemicals and antibodies

Curcumin, GTP, Pipes, sulfurhodamine B, colchicine, podophyllotoxin, vinblastine and 4′,6-diamidino-2-phenylindole (DAPI) were obtained from Sigma (St Louis, MO, USA). Phosphocellulose (P11) was purchased from Whatman (Maidstone, UK). P-6 resin was purchased from Bio-Rad (Hercules, CA, USA). The primary mouse monoclonal antibody against α-tubulin was from Sigma. Secondary antibody used in this study was goat antimouse IgG-Alexa-568 (Molecular Probes, Eugene, OR, USA).

Cell culture and proliferation assay

HeLa and MCF-7 cells were grown in minimal essential medium (Himedia, Mumbai, India) supplemented with 10% (v/v) fetal bovine serum, kanamycin (0.1 $mg \cdot mL^{-1}$), penicillin G (100 $units \cdot mL^{-1}$), and sodium bicarbonate (1.5 $mg \cdot mL^{-1}$) at 37 °C in 5% CO_2. Cell proliferation was determined by a standard sulforhodamine B assay as described previously [36]. Cells were incubated with different concentrations of curcumin, vinblastine and colchicine for one cell cycle (HeLa; 20 h, and MCF-7; 48 h) before fixation and staining with sulforhodamine B.

Immunofluorescence microscopy

Immunofluorescence microscopy was performed as described previously [24]. Briefly, cells were seeded on coverslips at a density of 25 000 cells per well in 24-well plates. Cells were fixed and nonspecific antibody binding sites were blocked by incubating with 2% BSA in NaCl/P_i at 37 °C for 15 min. Further, cells were incubated for 2 h at 37 °C with antiα-tubulin IgG (1 : 150 dilution) followed by a 1 : 100 dilution of Alexa568-conjugated secondary antibody. Then, the coverslips were rinsed with 2% BSA/NaCl/P_i for 10 min and incubated with DAPI (1 $\mu g \cdot mL^{-1}$) for 30 s. Images were taken by using a Nikon (Kanagawa, Japan) inverted microscope (TE2000) with a 40× objective and analyzed by IMAGE PRO PLUS software (Media Cybernetics, Silver Spring, MD, USA).

Purification of tubulin

Goat brain microtubule protein was isolated by two cycles of polymerization and depolymerization in the presence of 1 M glutamate and 10% (v/v) dimethylsulfoxide in the assembly buffer (25 mM Pipes, pH 6.8, 3 mM $MgSO_4$, 1 mM

EGTA, 1 mM GTP, 1.0 M monosodium glutamate, pH 6.8) [37]. MAP-free tubulin was purified from the microtubule protein by phosphocellulose chromatography [25]. Protein concentration was determined by the method of Bradford using BSA as standard [38].

Spectral measurements

Absorbance measurements were performed in a JASCO (Tokyo, Japan) V-530 UV-visible spectrophotometer using a cuvette of 1 cm path length. All fluorescence measurements were performed using a fluorescence spectrophotometer (JASCO FP-6500) equipped with a constant temperature water-circulating bath. To minimize the inner filter effects at high curcumin concentrations, a 0.3 cm path length cuvette was used for all fluorescence measurements. The inner filter effects were corrected using the formula

$$F_{corrected} = F_{observed} \times \text{antilog}(A_{excitation} + A_{emission})/2$$

Inhibition of purified tubulin assembly by curcumin

The kinetics of tubulin polymerization was monitored by 90° light scattering at 550 nm using a fluorescence spectrophotometer [26]. Tubulin (12 μM) was mixed with different concentrations of curcumin (0–100 μM) in the assembly buffer and the assembly reaction was initiated by incubating the sample at 37 °C. The effect of curcumin on the polymerized tubulin was determined by sedimentation. The microtubule polymers were collected by sedimentation (128 000 ***g***) for 40 min at 32 °C. The tubulin concentration in the pellet was determined by Bradford method [38].

Electron microscopy

Tubulin (12 μM) was polymerized in the absence and presence of curcumin as described above. Microtubules were fixed with prewarmed 0.5% glutaraldehyde for 5 min. Samples (20 μL) were applied to carbon-coated electron microscope grids (300 mesh size) for 30 s and blotted dry. The grids were subsequently negatively stained with 1% uranyl acetate solution for 30 s and air-dried. The samples were viewed with a Tecnai $G^2$12 electron microscope (FEI, Eindhoven, the Netherlands).

Estimation of tubulin aggregate size

Dynamic light scattering was used to determine the size of tubulin aggregates in the presence of curcumin. Tubulin was thawed and sedimented at 128 000 ***g*** to remove aggregates. Tubulin (10 μM) was incubated in the absence and presence of different concentration of curcumin for 10 min at 4 °C. The scattered light intensity was monitored at 25 °C at an angle of 90° using a Zeta Plus Analyzer (Brookhaven Instruments Corporation, Holtsville, NY, USA). A 1.0 cm path length quartz cuvette was used for the experiment.

Stoichiometry of tubulin–curcumin complex incorporation into microtubules

To measure the incorporation of tubulin–curcumin complex into microtubule polymers, first tubulin (40 μM) was incubated with 80 μM curcumin for 10 min at 4 °C to form tubulin–curcumin complex. The mixture was passed through a P-6 size exclusion column at 4 °C to separate the unbound curcumin. Tubulin containing fractions were centrifuged at 4 °C for 20 min at 128 000 ***g*** and supernatants were used for further experiments. Various concentrations of tubulin–curcumin complex with unlabelled tubulin (final concentrations of tubulin of 10 μM) were allowed to polymerize in the assembly buffer at 37 °C for 40 min. Polymers were collected by centrifugation (128 000 ***g***) at 32 °C for 40 min. Pellets were washed with prewarmed 1 M glutamate buffer. Pellets were dissolved in buffer A (25 mM Pipes, pH 6.8, 3 mM $MgSO_4$ and 1 mM EGTA). Curcumin concentration was determined by measuring absorbance at 425 nm and protein concentration was determined by the Bradford method [38]. The background absorbance of curcumin was determined using BSA instead of tubulin and it was found to be less than 1% of the signal.

Measurement of GTPase activity

The standard malachite green sodium molybdate assay was used to estimate the amount of P_i released during GTP hydrolysis [39]. Microtubule protein (1.8 $mg{\cdot}mL^{-1}$) was incubated with 50 μM curcumin at 0 °C for 10 min. Then polymerization reactions were initiated by incubating the samples at 37 °C with 1 mM GTP. At the desired time points, 50 μL samples were removed and processed for the malachite green assay as described previously [25,39].

Titration of tubulin sulfhydryl groups

The sulfhydryl-specific reagent DTNB complexes with thiol groups in tubulin [24,25]. The rate and extent of sulfhydryl-group modification by DTNB in the absence and presence of curcumin were monitored by measuring the absorbance changes at 412 nm [24,25]. Tubulin–curcumin complex were prepared as described in the previous experiment of copolymerization. The number of sulfhydryl groups modified after 40 min of reaction was determined by using a molar extinction coefficient of 12 000 for DTNB at 412 nm.

Binding measurements by fluorometric titration

Fluorescence of curcumin

The increased curcumin fluorescence at 495 nm upon binding to tubulin was used to determine the affinity of curcumin with tubulin. Tubulin (2.0 μM) was allowed to react with varying concentrations of curcumin (0.5–10 μM) in buffer A at 25 °C for 40 min. The excitation and emission wavelength were 425 nm and 495 nm, respectively. The dissociation constant (K_d) and number of curcumin binding sites (n) on the tubulin were determined by the method described by Hiratsuka [40]. Briefly, the fluorescence of curcumin was measured in the presence (F) and absence (F_o) of tubulin, and the ratio of fluorescence (F/F_o) was used to calculate $[curcumin]_{bound}$ from

$$[curcumin]_{bound} = [curcumin]_{total}/Q - 1(F/F_o - 1)$$

where, Q is the enhancement factor of curcumin fluorescence for bound ligand. Q was measured by titrating a fixed amount of curcumin (1.0 μM), with increasing amounts of the tubulin in a concentration range of 2–12 μM. A double-reciprocal plot of total protein concentration versus observed fluorescence was extrapolated to infinite protein concentration in order to determine the value of Q. Enhancement factor, Q, of curcumin was 107. The amount of free curcumin is obtained from the difference of the total curcumin and calculated bound curcumin. The data were analyzed in terms of the Scatchard equation [41],

$$B/[F]T = n/K_d - B/K_dT$$

Where, [F] is the free curcumin concentration, B and T are amounts of bound curcumin and total tubulin, respectively, n is the number of binding sites, and K_d is the dissociation constant for the tubulin–curcumin complex.

Quenching of the protein fluorescence

We used intrinsic tryptophan fluorescence of tubulin to measure the binding affinity of curcumin to tubulin. Tubulin (2 μM) was incubated with varying concentrations of curcumin (0–10 μM) at 25 °C for 40 min. The fluorescence measurements were performed using 295 nm as the excitation wavelength. The data were analyzed as described previously [24,25]. The dissociation constant (K_d) was determined using the relationship, $1/B = 1 + K_d/F$, where F represents free curcumin concentration and $F = C–B$ [Y], where C is total concentration of curcumin and [Y] is the molar concentration of ligand binding sites assuming a single binding site per tubulin dimer [24,25].

Competitive binding assay

The ability of curcumin to compete with colchicine, podophyllotoxin and vinblastine for binding to tubulin was assessed by measuring the change in the tubulin–curcumin complex fluorescence. Tubulin (2 μM) was incubated with different concentrations of colchicine and podophyllotoxin (1–25 μM) for 1 h at 37 °C. For vinblastine, tubulin (2 μM) was incubated with different concentrations (5–50 μM) of vinblastine at room temperature for 20 min. Then 10 μM curcumin was added to all reaction mixtures and spectra were recorded after 30 min incubation at 25 °C by exciting the samples at 425 nm.

Binding of curcumin to preformed tubulin–colchicine or tubulin–podophyllotoxin complex

Tubulin (3 μM) was incubated in the absence and presence of 100 μM colchicine or podophyllotoxin for 45 min at 37 °C. Then, 3 μM curcumin was added to the reaction mixtures and incubated for an additional 15 min. The dissociation constants for colchicine and podophyllotoxin interactions with tubulin are reported to be 0.5 μM and 0.6 μM, respectively [42,43]. Therefore, under the experimental conditions used, tubulin would be completely liganded with colchicine or podophyllotoxin. The reaction mixtures were excited at 425 nm and the emission spectra were recorded as described previously.

Statistical analysis

Data was analyzed using one-way ANOVA. Data is expressed as mean ± SE.

Acknowledgements

We wish to thank Sophisticated Analytical Instrument Facility (SAIF), IIT Bombay for electron microscopy facility. We thank Renu Mohan and Dipti Rai for critical reading of the manuscript. The work is supported in part by grant from the Department of Biotechnology, Government of India. DP is supported by Swarnajayanti Fellowship from the Department of Science and Technology, Government of India.

References

1 Singletary K (2000) Diet, natural products and cancer chemoprevention. *J Nutr* **130**, 465–466.
2 Surh YJ (2003) Cancer chemoprevention with dietary phytochemicals. *Nat Rev Cancer* **3**, 768–780.
3 Dorai T & Aggarwal BB (2004) Role of chemopreventive agents in cancer therapy. *Cancer Lett* **215**, 129–140.
4 Sarkar FH & Li Y (2004) Cell signaling pathways altered by natural chemopreventive agents. *Mutat Res* **555**, 53–64.

5 Li JK & Lin-Shia SY (2001) Mechanisms of cancer chemoprevention by curcumin. *Proc Natl Sci Counc Repub China B* **25**, 59–66.
6 Ruby AJ, Kuttan G, Babu KD, Rajasekharan KN & Kuttan R (1995) Anti-tumor and antioxidant activity of natural curcuminoids. *Cancer Lett* **94**, 79–83.
7 Kawamori T, Lubet R, Steele VE, Kelloff GJ, Kaskey RB, Rao CV & Reddy BS (1999) Chemopreventive effect of curcumin, a naturally occurring anti-inflammatory agent, during the promotion/progression stages of colon cancer. *Cancer Res* **59**, 597–601.
8 Cheng AL, Hsu CH, Lin JK, Hsu MM, Ho YF, Shen TS, Ko JY, Lin JT, Lin BR, Ming-Shiang W *et al* (2001) Phase I clinical trial of curcumin, a chemopreventive agent, in patients with high-risk or pre-Malignant lesions. *Anticancer Res* **21**, 2895–2900.
9 Aggarwal BB, Kumar A & Bharti AC (2003) Anticancer potential of curcumin: preclinical and clinical studies. *Anticancer Res* **23**, 363–398.
10 Simon A, Allais DP, Duroux JL, Basly JP, Durand-Fontanier S & Delage C (1998) Inhibitory effect of curcuminoids on MCF-7 cell proliferation and structure-activity relationships. *Cancer Lett* **129**, 111–116.
11 Chauhan DP (2002) Chemotherapeutic potential of curcumin for colorectal cancer. *Curr Pharm Des* **81**, 695–706.
12 Jee SH, Shen SC, Tseng CR, Chin HC & Kuo ML (1998) Curcumin induces a p53-dependent apoptosis in human basal cell carcinoma cells. *J Invest Dermatol* **111**, 656–661.
13 Dorai T, Cao YC, Dorai B, Buttyan R & Katz AE (2001) Therapeutic potential of curcumin in human prostate cancer. III. Curcumin inhibits proliferation, induces apoptosis, and inhibits angiogenesis of LNCaP prostate cancer cells *in vivo*. *Prostate* **47**, 293–303.
14 Gururaj AE, Belakavadi M, Venkatesh DA, Marme D & Salimath BP (2002) Molecular mechanisms of anti-angiogenic effect of curcumin. *Biochem Biophys Res Commun* **297**, 934–942.
15 Park MJ, Kim EH, Park IC, Lee HC, Woo SH, Lee JY, Hong YJ, Rhee CH, Choi SH, Shim BS *et al* (2002) Curcumin inhibits cell cycle progression of immortalized human umbilical vein endothelial (ECV304) cells by up-regulating cyclin-dependent kinase inhibitor, p21WAF1/CIP1, p27KIP1 and p53. *Int J Oncol* **21**, 379–383.
16 Anuchapreeda S, Leechanachai P, Smith MM, Ambudkar SV & Limtrakul PN (2002) Modulation of P-glycoprotein expression and function by curcumin in multidrug-resistant human KB cells. *Biochem Pharmacol* **64**, 573–582.
17 Holy JM (2002) Curcumin disrupts mitotic spindle structure and induces micronucleation in MCF-7 breast cancer cells. *Mutat Res* **518**, 71–84.
18 Choudhuri T, Pal S, Das T & SaG (2005) Curcumin selectively induces apoptosis in deregulated cyclin D1 expressed cells at G2 phase of cell cycle in a p53-dependent manner. *J Biol Chem* **280**, 20059–20068.
19 Van Erk MJ, Teuling E, Staal YC, Huybers S, Van Bladeren PJ, Aarts JM & Van Ommen B (2004) Time- and dose-dependent effects of curcumin on gene expression in human colon cancer cells. *J Carcinog* **3**, 8–25.
20 Desai A & Mitchison TJ (1997) Microtubule polymerization dynamics. *Annu Rev Cell Dev Biol* **13**, 83–117.
21 Jordan MA & Wilson L (2004) Microtubules as a target for anticancer drugs. *Nat Rev Cancer* **4**, 253–265.
22 Bhalla KN (2003) Microtubule-targeted anticancer agents and apoptosis. *Oncogene* **22**, 9075–9086.
23 Dumontet C (2000) Mechanisms of action and resistance to tubulin-binding agents. *Expert Opin Invest Drugs* **9**, 779–788.
24 Gupta K, Bishop J, Peck A, Brown J, Wilson L & Panda D (2004) Antimitotic antifungal compound benomyl inhibits brain microtubule polymerization and dynamics and cancer cell proliferation at mitosis, by binding to a novel site in tubulin. *Biochemistry* **43**, 6645–6655.
25 Gupta K & Panda D (2002) Perturbation of microtubule polymerization by quercetin through tubulin binding: a novel mechanism of its antiproliferative activity. *Biochemistry* **41**, 13029–13038.
26 Gaskin F, Cantor CR & Shelanski ML (1974) Turbidimetric studies of the *in vitro* assembly and disassembly of porcine neurotubules. *J Mol Biol* **89**, 737–755.
27 D'Amato RJ, Lin CM, Flynn E, Folkman J & Hamel E (1994) 2-Methoxyestradiol, an endogenous mammalian metabolite, inhibits tubulin polymerization by interacting at the colchicine site. *Proc Natl Acad Sci USA* **91**, 3964–3968.
28 Zhou J, Panda D, Landen JW, Wilson L & Joshi HC (2002) Minor alteration of microtubule dynamics causes loss of tension across kinetochore pairs and activates the spindle checkpoint. *J Biol Chem* **277**, 17200–17208.
29 Panda D, Miller HP, Islam K & Wilson L (1997) Stabilization of microtubule dynamics by estramustine by binding to a novel site in tubulin: a possible mechanistic basis of its antitumor action. *Proc Natl Acad Sci USA* **94**, 10560–10564.
30 Jordan MA, Walker D, de Arruda M, Barlozzari T & Panda D (1998) Suppression of microtubule dynamics by binding of cemadotin to tubulin: possible mechanism for its antitumor action. *Biochemistry* **37**, 17571–17578.
31 Panda D, Rathinasamy K, Santra MK & Wilson L (2005) Kinetic suppression of microtubule dynamic instability by griseofulvin: implications for its possible use in the treatment of cancer. *Proc Natl Acad Sci USA* **102**, 9878–9883.

32 Hamel E, Lin CM, Flynn E & D'Amato RJ (1996) Interactions of 2-Methoxyestradiol, an endogenous mammalian metabolite, with unpolymerized tubulin and with tubulin polymers. *Biochemistry* **35**, 1304–1310.
33 Folkman J (2002) Role of angiogenesis in tumor growth and metastasis. *Semin Oncol* **6**, 15–18.
34 Mabjeesh NJ, Escuin D & LaVallee TM (2003) 2ME2 inhibits tumor growth and angiogenesis by disrupting microtubules and dysregulating HIF. *Cancer Cell* **3**, 363–375.
35 Pollmann C, Huang X & Mall J (2001) The constitutive photomorphogenesis 9 signalosome directs vascular endothelial growth factor production in tumor cells. *Cancer Res* **61**, 8416–8421.
36 Skehan P, Storeng R & Scudiero D (1990) New colorimetric cytotoxicity assay for anticancer-drug screening. *J Natl Cancer Inst* **82**, 1107–1112.
37 Hamel E & Lin CM (1981) Glutamate-induced polymerization of tubulin: characteristics of the reaction and application to the large-scale purification of tubulin. *Arch Biochem Biophys* **209**, 29–40.
38 Bradford MM (1976) A rapid and sensitive method for the quantitation of microgram quantities of protein utilizing the principle of protein-dye binding. *Anal Biochem* **72**, 248–254.
39 Lanzetta PA, Alvarez LJ, Reinach PS & Candia OA (1979) An improved assay for nanomole amounts of inorganic phosphate. *Anal Biochem* **100**, 95–97.
40 Hiratsuka TA (1985) Chromophoric and fluorescent analog of GTP, 2′, 3′-O-(2,4,6-trinitrocyclohexadienylidene) -GTP, as a spectroscopic probe for the GTP inhibitory site of liver glutamate dehydrogenase. *J Biol Chem* **260**, 4784–4790.
41 Scatchard G (1949) The attractions of proteins for small molecules ions. *Ann N Y Acad Sci* **51**, 660–672.
42 Panda D, Roy S & Bhattacharyya B (1992) Reversible dimer dissociation of tubulin S and tubulin detected by fluorescence anisotropy. *Biochemistry* **31**, 9709–9716.
43 Cortese F, Bhattacharyya B & Wolff J (1977) Podophyllotoxin as a probe for the colchicine binding site of tubulin. *J Biol Chem* **252**, 1134–1140.